

Time-Course of Vibratory Adaptation and Recovery in Cutaneous Mechanoreceptive Afferents

Y. Y. Leung,³ S. J. Bensmaïa,^{1,2} S. S. Hsiao,^{1,2,3} and K. O. Johnson^{1,2,3}

¹Krieger Mind/Brain Institute, ²Department of Neuroscience, and ³Department of Biomedical Engineering, Johns Hopkins University, Baltimore, Maryland

Submitted 3 January 2005; accepted in final form 11 July 2005

Leung, Y. Y., S. J. Bensmaïa, S. S. Hsiao, and K. O. Johnson. Time-course of vibratory adaptation and recovery in cutaneous mechanoreceptive afferents. *J Neurophysiol* 94: 3037–3045, 2005; doi:10.1152/jn.00001.2005. Extended suprathreshold vibratory stimulation applied to the skin results in a desensitization of cutaneous mechanoreceptive afferents. In a companion paper, we describe the dependence of the threshold shift on the parameters of the adapting stimulus and discuss neural mechanisms underlying afferent adaptation. Here we describe the time-course of afferent adaptation and recovery. We found that absolute and entrainment thresholds rise and fall exponentially during adaptation and recovery with time constants that vary with fiber type. Slowly adapting type I (SA1) afferents adapt most rapidly, and pacinian (PC) afferents adapt most slowly, whereas rapidly adapting (RA) afferents exhibit intermediate rates of adaptation; SA1 fibers also recover more rapidly from adaptation than RA and PC fibers. We also showed that threshold adaptation is accompanied by a shift in the timing of the spikes within individual cycles of the adapting stimulus (i.e., a shift in the impulse phase). We invoked an integrate-and-fire model to explore possible mechanisms underlying afferent adaptation. Finally, we found that the time-course of afferent adaptation is more rapid than that of its psychophysical counterpart, as is the time-course of recovery from adaptation, suggesting that central factors play a role in the psychophysical phenomenon.

INTRODUCTION

Extended exposure to a suprathreshold vibratory stimulus applied to the skin results in a reversible decrement in the sensitivity of cutaneous mechanoreceptive afferents (Bensmaïa et al. 2005). In a companion paper, we discussed the dependence of afferent adaptation on the parameters of the conditioning stimulus. Specifically, we showed that the shift in the absolute (I_0) and entrainment (I_1) thresholds increases as the adapting amplitude or frequency increases. Furthermore, as the effects of adaptation on I_0 and I_1 were found to be approximately additive, particularly in rapidly adapting (RA) fibers, we speculated that adaptation operates on the spiking threshold of the afferent rather than on the transducer sensitivity of the receptor.

The time-course along which afferent adaptation and recovery operate is largely unknown, in part because the phenomenon itself has been difficult to study for reasons discussed in the companion paper (Bensmaïa et al. 2005). Recording from RA afferents in monkeys and cats, Whitsel et al. (2000) observed a slight drop in mean spike rate within the first few seconds of a vibratory stimulus. The observed decline in responsiveness was accompanied by a slight increase in the phase angle of the entrained response within the first 100–500 ms of the stimulus. Recording the responses from PC fibers in cat

mesentery, O'Mara et al. (1988) found that the spike rates recovered to their preadaptation levels along approximately exponential time-courses, with time constants <30 s. In this study, we investigated the time-course of adaptation in slowly adapting type I (SA1), RA, and pacinian (PC) fibers using two indices of afferent sensitivity: 1) absolute and entrainment thresholds measured using a novel tracking algorithm described in Bensmaïa et al. (2005) and 2) the phase at which afferents produce a spike within each cycle of the adapting stimulus. We show that the observed rates of adaptation and recovery are compatible with predictions derived from a simple integrate-and-fire model. Finally, we compare the time-courses of afferent adaptation and recovery with previously reported time-courses of psychophysical adaptation and recovery and conclude that central factors must also play a role in the psychophysical phenomenon of vibratory adaptation.

METHODS

The methods and stimuli are described in detail in a companion paper (Bensmaïa et al. 2005). Briefly, single unit recordings were obtained from the ulnar and median nerves of five macaque monkeys (*Macaca mulatta*) using standard methods (Talbot et al. 1968). Each unit was classified as SA1, RA, or PC according to its responses to step indentations and vibratory stimulation (Freeman and Johnson 1982a,b; Talbot et al. 1968). The stimulator consisted of a feedback-controlled mechanical vibrator (Chubbuck 1966) that drove a 1-mm-diam probe, the tip of which was glued to the skin surface at the point of maximum sensitivity with cyanoacrylate glue. The probe vibrated normally to the surface of the skin around the skin's resting position. Each stimulus run comprised a preadaptation, an adaptation, and a recovery period. A test stimulus, 1 s long, was presented every 4 s. The 3-s interstimulus interval was empty during the preadaptation and recovery periods and was filled with the adapting stimulus during the adaptation period. The amplitude (A_a) and frequency (F_a) of the adapting stimulus and the frequency of the test stimulus (F_t) varied from run to run, as did the durations of the adaptation and recovery periods. Adapting and test frequencies were selected to span the range over which each class of afferent was maximally responsive: 10, 30, and 60 Hz for SA1; 30, 60, and 100 Hz for RA; and 60, 100, and 300 Hz for PC fibers (also 200 Hz on some runs). Adapting amplitudes ranged from 1 to 25 times the unadapted absolute threshold. The durations of the adaptation and recovery periods ranged from 1 to 16 min. Reported amplitudes are zero-to-peak microns.

Threshold shifts

Absolute and entrainment thresholds of the afferents were measured on-line using a tracking algorithm, described in detail in the

Address for reprint requests and other correspondence: S. J. Bensmaïa, 3400 N. Charles St., Krieger 338, Baltimore, MD 21218 (E-mail: sliman@jhu.edu).

The costs of publication of this article were defrayed in part by the payment of page charges. The article must therefore be hereby marked "advertisement" in accordance with 18 U.S.C. Section 1734 solely to indicate this fact.

companion paper. The averages of the last five I_0 and I_1 estimates from the adaptation period were used to estimate the adapted thresholds. Similarly, the averages of the last five I_0 and I_1 measurements from the recovery period provided estimates of the recovered thresholds. The time-course of vibrotactile adaptation and recovery was characterized post hoc as a series of exponential functions. Preadaptation thresholds were fitted with a horizontal line, because thresholds theoretically remained constant during this period. Thresholds from the adaptation period were fitted with the method of least squares to an exponential function of the form

$$I(t) = I(0) + \delta(1 - e^{-\frac{(t-t_a)}{\tau_a}}), \quad t_a \leq t \leq t_r \quad (1)$$

where $I(t)$ is the threshold (I_0 or I_1) at time t , $I(0)$ is the unadapted, δ is the threshold shift, t_a is the time of onset of the adapting stimulus, and τ_a is the adaptation time constant. Similarly, recovering thresholds were fit to an exponential of the form

$$I(t) = I(0) + \delta - \gamma(1 - e^{-\frac{(t-t_r)}{\tau_r}}), \quad t \geq t_r \quad (2)$$

where t_r is the beginning of recovery period (time of offset of the adapting stimulus), γ is the degree of threshold recovery, and τ_r is the recovery time constant. (Note that τ_a , τ_r , δ , and γ are free parameters and $\delta = \gamma$ if thresholds recover to preadaptation levels.) As can be seen from plots of thresholds versus time (Figs. 1–3), shifts in thresholds during the adaptation and recovery periods are well described by exponential functions.

Time constants are meaningless in the absence of a threshold shift, and time constant estimates are unreliable for small threshold shifts. Accordingly, time constants were computed only for stimulus runs in which the threshold shift exceeded 20% of the unadapted threshold. Because PC afferents are relatively unsusceptible to adaptation, fewer runs with PC fibers met the threshold shift criterion. As a result, fewer estimates of time constants were obtained from these afferents than from SA1 and RA afferents.

Phase shift

Along with increases in threshold, adaptation also causes a progressive shift in the phase at which the afferent produces a spike

within each stimulus cycle: as the sensitivity of the receptor declines, it takes longer for the receptor potential to reach threshold and the impulse phase progressively increases. Note that accurate estimates of phase shift require near-perfect entrainment of the neural response as impulse phase is also affected by the immediate spiking history of the afferent (Freeman and Johnson 1982b). Specifically, the impulse occurs later in a stimulus cycle if the previous cycle evoked an impulse than if it did not (Freeman and Johnson 1982b). If every stimulus cycle evokes the same number of impulses, systematic shifts in impulse phase are caused by changes in the excitability of the neuron, i.e., to adaptation, and thus can yield an additional estimate of the time course of adaptation.

We measured the phase adaptation, i.e., the progressive shift in impulse phase during the adaptation period, for stimulus runs on which afferent responses were entrained to the adapting stimulus (i.e., produced the same number of spikes on each stimulus cycle). The criterion for entrainment was that the afferent fire a given number of spikes (typically 1, but sometimes 2 or even 3) on 80% or more of adapting stimulus cycles over the course of the adaptation period. For each run meeting this criterion, the phase of the first spike produced on each cycle of the adapting stimulus was measured, along with its time of occurrence within the adapting period. The impulse phase was the time of the first spike produced in a given cycle, normalized by the period of the cycle (i.e., $1/F_a$) and multiplied by 360° . The phases of the spikes evoked during the first few cycles of the stimulus in each adapting interval were not included in the analysis because impulse phase shifts rapidly before reaching steady state (i.e., a state changing over the span of seconds) for reasons unrelated to adaptation (but that are beyond the scope of this study). We show here that phase adaptation accompanies threshold shift and, like threshold shift, progresses along an exponential time-course. Thus time constants of adaptation could be independently estimated using the procedure described above then compared with those obtained using threshold shifts.

RESULTS

Results obtained from 9 SA1, 11 RA, and 11 PC fibers are reported here. The magnitude of the threshold shift and its

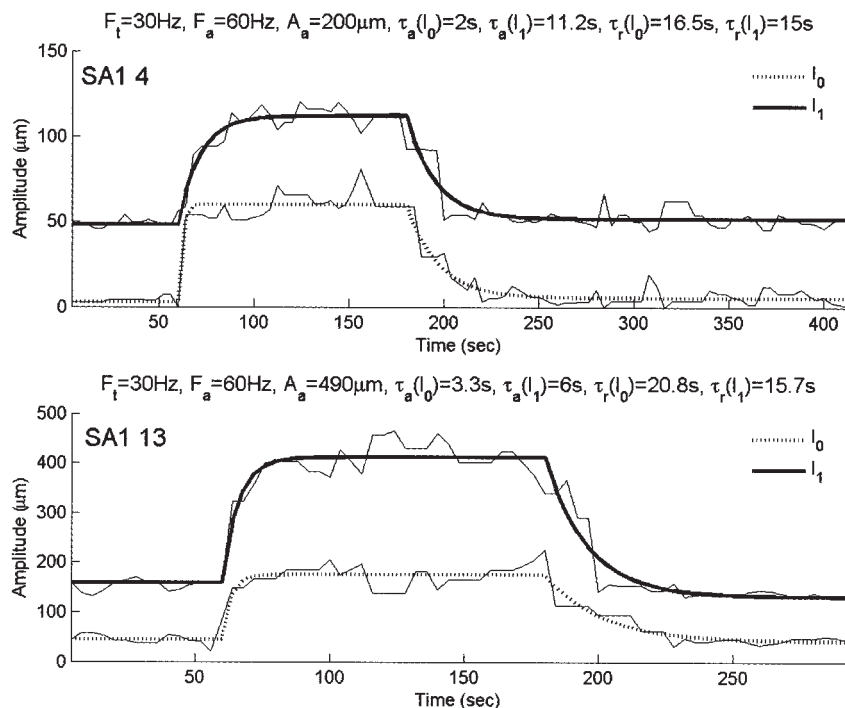


FIG. 1. Time-course of adaptation and recovery for 2 typical SA1 afferents. Stimulus parameters and time constants are shown above each plot. Thin lines, thresholds estimated from the tracking algorithm; thick dotted and solid lines, fitted exponential functions. F_t , test frequency; F_a , adaptation frequency; A_a , adaptation amplitude; τ_a , adaptation time constant; τ_r , recovery time constant.

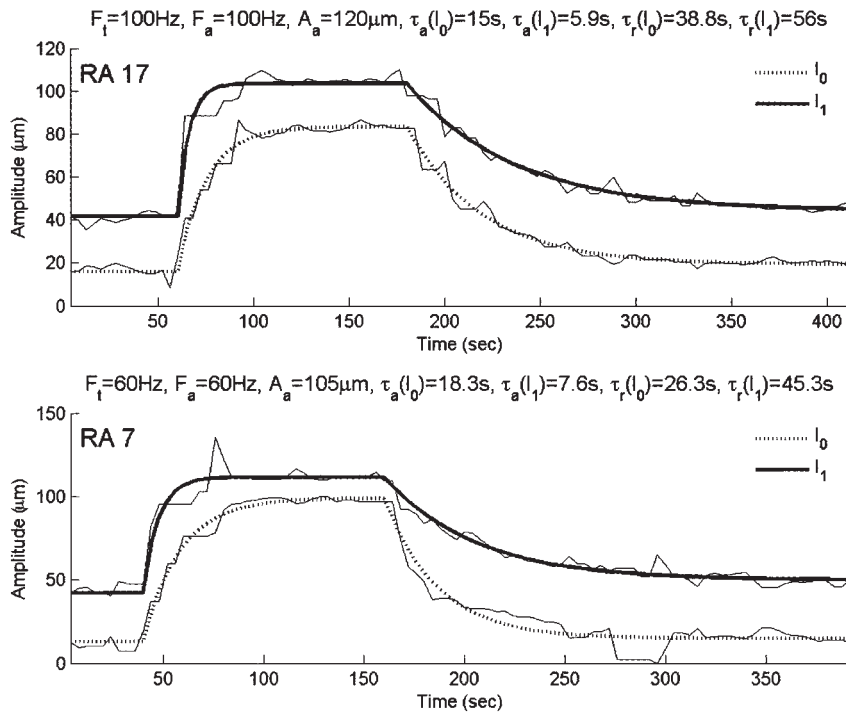


FIG. 2. Time-course of adaptation and recovery for 2 typical RA afferents. Conventions as in Fig. 1.

dependence on stimulus parameters are discussed in a companion paper (Bensmaïa et al. 2005). In this paper, we discuss the time-course of adaptation and recovery.

Time-course of the threshold adaptation

Figures 1–3 show time-courses of adaptation and recovery obtained from typical SA1, RA, and PC afferents. SA1 and RA thresholds shifted rapidly upon onset of the adapting stimulus and remained at their adapted levels throughout the remainder

of the adapting period. On the other hand, PC thresholds often had not stabilized by the end of adaptation periods lasting 2, 4, and sometimes even 8 min. SA1 afferents tended to recover most rapidly, whereas RA and PC afferents recovered at similar, slower rates. Differences in the rates of recovery across fiber types were less pronounced than differences in the rates of adaptation.

PC fibers are exquisitely sensitive to mechanical stimulation, often exhibiting submicron absolute thresholds. Furthermore, PC fibers are relatively unsusceptible to adaptation (Bensmaïa

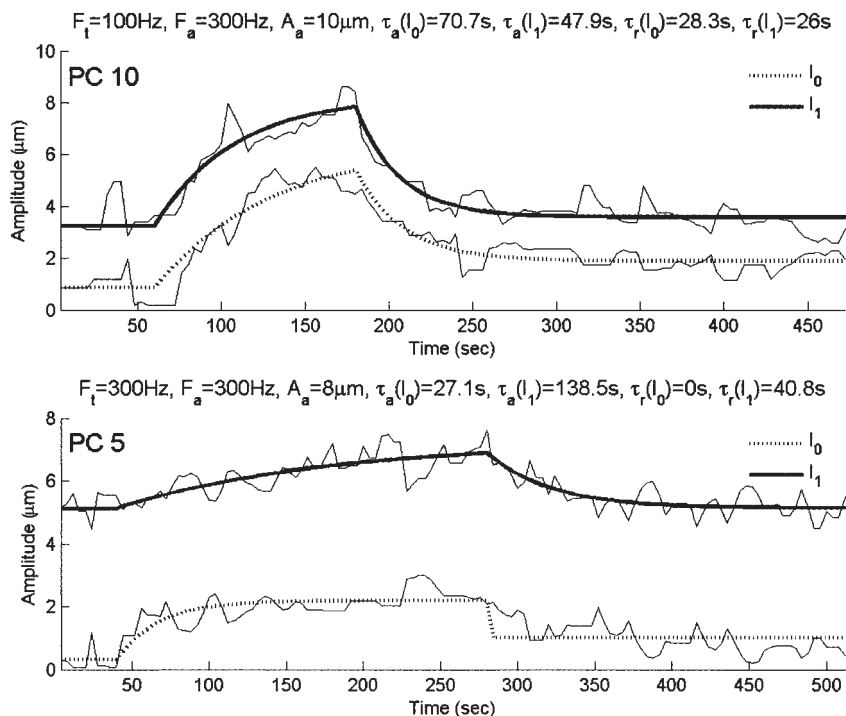


FIG. 3. Time-course of adaptation and recovery for 2 typical PC afferents. Conventions as in Fig. 1.

et al. 2005). As a result, the recovered thresholds obtained from these afferents were relatively noisy. More reliable estimates of the time-course of PC adaptation were obtained by estimating the time-course of the shift in impulse phase during the adaptation period.

Time-course of adaptation

The left panels of Fig. 4 show the distributions of threshold adaptation time constants for the three types of afferents. SA1 fibers tended to adapt most quickly, with mean time constants of 11 and 9 s for I_0 and I_1 . RA fibers had somewhat longer adaptation time constants ($\bar{\tau}_{I_0}$: 17.9 s; $\bar{\tau}_{I_1}$: 13.2 s). PC fibers were the slowest to adapt ($\bar{\tau}_{I_0}$: 41.8 s; $\bar{\tau}_{I_1}$: 28.1 s; Fig. 4, left). SA1 I_0 and I_1 adaptation time constants were not significantly different (paired t -test, $P > 0.05$). RA and PC I_0 adaptation time constants were 50% longer than their I_1 counterparts, but that difference was only significant for RA afferents (paired t -test, $P < 0.01$); the difference was not significant for PC fibers, likely because of the high degree of variability in the time constants obtained from these afferents.

Time-course of recovery

The right panels of Fig. 4 show the distributions of recovery time constants for the three types of afferents. SA1 fibers recovered most rapidly, with mean time constants of 9.4 and 17.3 s for I_0 and I_1 thresholds, respectively. Recovery time constants for RA fibers ($\bar{\tau}_{I_0}$: 27 s; $\bar{\tau}_{I_1}$: 26.6 s), and PC afferents

($\bar{\tau}_{I_0}$: 20.9 s; $\bar{\tau}_{I_1}$: 29.6 s) were somewhat slower (Fig. 4, right). I_0 and I_1 recovery time constants were not significantly different from one another for both RA and PC fibers (paired t -test, $P > 0.05$). SA1 I_0 recovery time constants, on the other hand, were almost twice as fast as I_1 recovery time constants (paired t -test, $P < 0.001$).

Entrainment thresholds measured at the end of the recovery periods did not differ systematically from their preadaptation levels (Fig. 5). Preadaptation and recovered absolute thresholds exhibited greater variability than their I_1 counterparts, likely because of the fact that I_0 tended to be much smaller than I_1 and thus more susceptible to measurement noise. Overall, these results suggest that all three afferent types generally returned to their resting responsiveness within the allotted recovery periods (which ranged from 2 to 16 min for SA1 and RA fibers and from 4 to 16 min for PC fibers).

Comparing the time-courses of adaptation and recovery

SA1 I_1 recovery was slower than I_1 adaptation (t -test, $P < 0.001$), but the I_0 rates were not significantly different from one another. RA recovery tended to be slower than adaptation (Fig. 6) for both I_0 and I_1 (t -test, $P < 0.001$). Finally, PC adaptation and recovery time constants were not significantly different for both I_0 and I_1 (again, perhaps because of the variability of the PC time constants).

Dependence of time constants on stimulus parameters

In the previous analyses, we assumed adaptation and recovery time constants to be independent of the stimulus param-

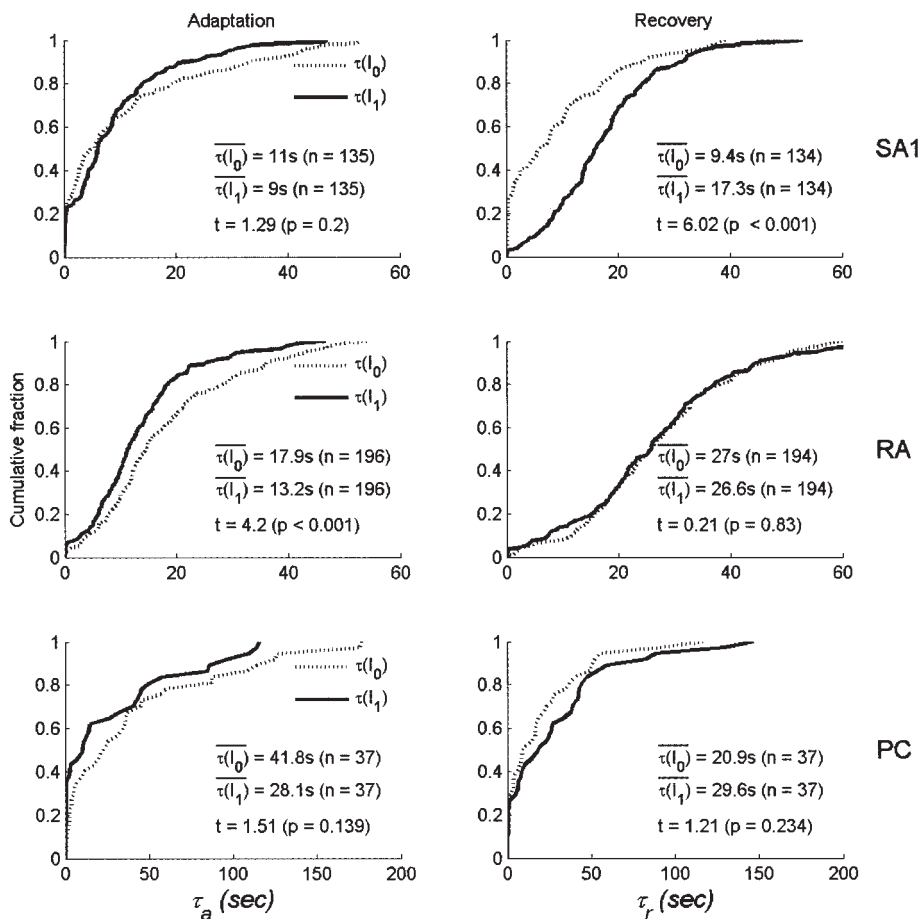


FIG. 4. Cumulative histograms of adaptation (left) and recovery (right) threshold time constants for all SA1, RA, and PC afferents and all stimulus conditions.

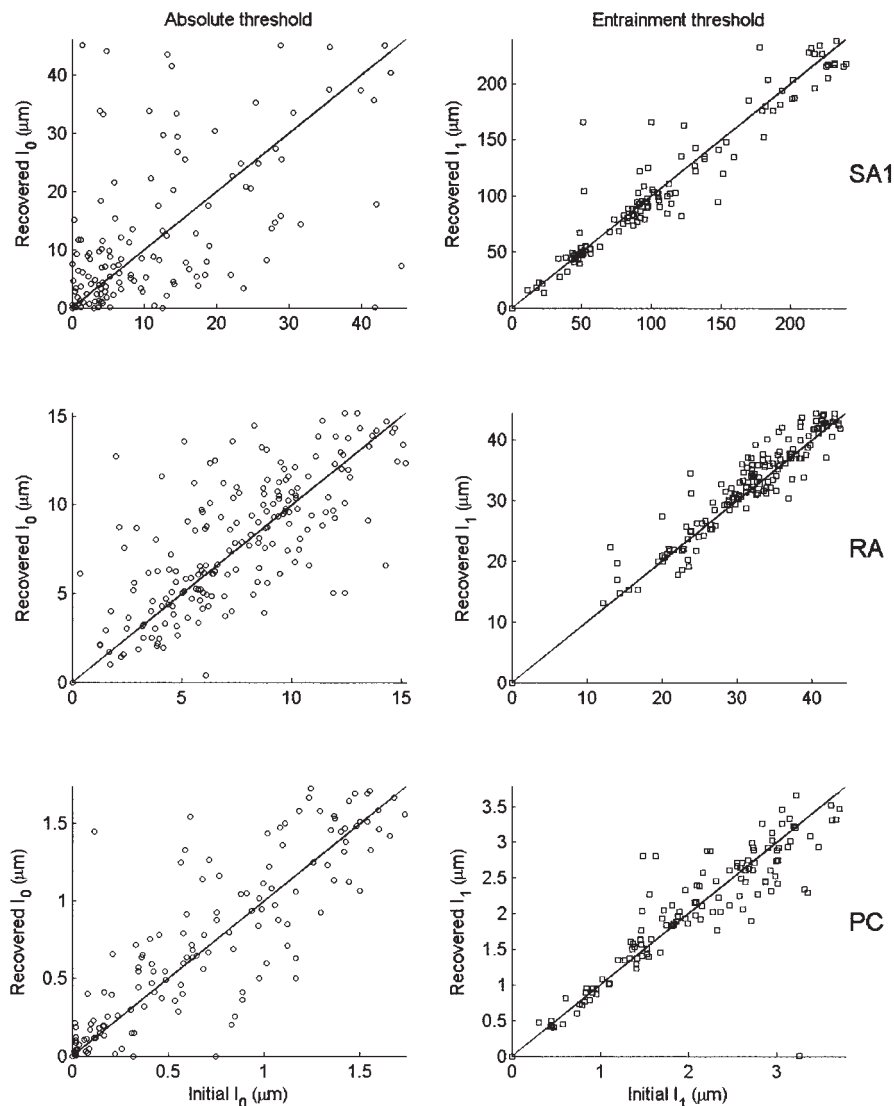


FIG. 5. Correspondence between the initial and final (recovered) I_0 and I_1 thresholds. I_0 correspondence seems more variable because the scale is generally magnified by a factor of 3 or more relative to the I_1 scale.

ters. To test this assumption, we performed an ANOVA on each type of time constant (adaptation and recovery, absolute, and entrainment threshold) with F_t , F_a , and A_a as covariates (with an additional factor to control for differences across fibers of a given type). Time constants were found to be largely independent of stimulus parameters, i.e., the effects of test and adapting frequency and adapting amplitude were generally nonsignificant ($\alpha = 0.05$). In the few cases in which there was a significant effect of a stimulus parameter on τ , the effect accounted for a negligible fraction of the variance in the time constants ($\eta_p^2 \leq 0.1$). These results suggest that the time constants are an inherent property of the afferent fibers themselves and are not stimulus-dependent. Given the inconsequentiality of these effects, they are not reported in detail here.

Time-course of phase adaptation

On stimulus runs in which the afferent response was entrained with the adapting stimulus, each cycle of the adapting stimulus contributed a data point to the estimate of the impulse phase adaptation time constant. Figure 7 shows the time-course of phase adaptation for one receptor of each type. For all three

afferent types, impulse phase increased exponentially with time. Figure 8 shows the cumulative histograms of phase adaptation time constants for the three fiber types. SA phase adaptation time constants were faster than their RA and PC counterparts ($t = 2.95$ and 3.98 for RA and PC fibers, respectively; $P < 0.01$). On the other hand, RA and PC phase adaptation time constants were not significantly different ($t = 1.77$, $P > 0.05$). Furthermore, the variability of these time constant estimates was much lower than that of their threshold shift counterparts, likely because of the fact that impulse phase could be estimated on each cycle of the adapting stimulus, whereas only one estimate of threshold was obtained on each adaptation trial. The median number of observations used to compute phase adaptation time constants was $\sim 4,500$ (mean, $\sim 7,000$), two orders of magnitude higher than the median number of adaptation trials per run (~ 30).

To test the dependency of phase adaptation time constants on stimulus parameters, an ANOVA was performed with adapting amplitude and frequency as factors. Similar to what was observed for the threshold time constants, neither stimulus parameter showed any relationship to the rate of phase adaptation for any of the three fiber types ($P > 0.05$).

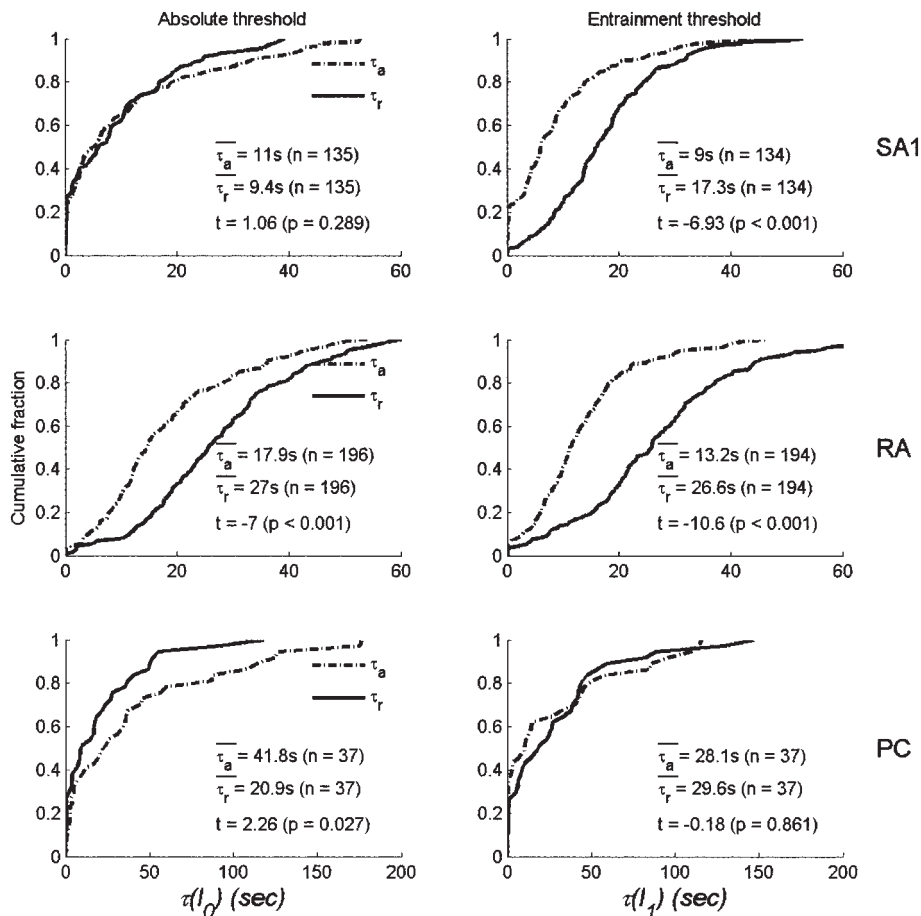


FIG. 6. Cumulative histograms of adaptation and recovery time constants for I_0 (left) and I_1 (right) thresholds for all 3 types of afferents. Conventions as in Fig. 4, in which the same data are presented in different pairings.

However, the asymptotic phase shift increased with the amplitude and frequency of the adapting stimulus, as did the absolute and entrainment thresholds. The relationship between the phase adaptation and threshold adaptation is explored in DISCUSSION.

DISCUSSION

Phase adaptation versus threshold shift

The time-course of adaptation was measured using two methods: one using thresholds and the other using impulse phase in entrained responses. We found the rates of adaptation measured using the two methods to be different, particularly for PC afferents (Table 1). Specifically, phase adaptation time constants were faster than their threshold shift counterparts for PC fibers. The discrepancies between the time constants measured using the two methods could be caused by measurement error or by differences in the mechanisms underlying the measured quantities.

To study the relationship between the time-course of threshold adaptation and that of phase adaptation, we invoke a simple integrate-and-fire model. The model, similar to the one described by Freeman and Johnson (1982b), is described in greater detail in a companion paper (Bensmaïa et al. 2005). Briefly, the function relating conductance to stimulus intensity is assumed to be linear with a slope determined by the transduction gain, k . T is the resting spiking threshold of the receptor, and ΔT is the residual increment in spiking threshold

on a stimulus cycle after a cycle on which a spike was produced (reflecting the relative refractoriness of the spiking mechanism). When the afferent response is entrained with the stimulus, the impulse phase is proportional to the instantaneous threshold of the afferent and inversely proportional to the transducer gain. Thus

$$\theta_s \propto \frac{T + \Delta T}{k} \quad (3)$$

Furthermore

$$I_1 \propto \frac{T + \Delta T}{k} \quad (4)$$

(Bensmaïa et al. 2005). According to the model, the phase at which a spike is produced within each stimulus cycle is proportional to the entrainment threshold, and the two should have identical time-courses, which is precisely the case for SA1 and RA fibers (Table 1).

On the other hand, PC threshold adaptation time constants were substantially longer than their phase adaptation counterparts. This discrepancy is likely because of measurement error in the threshold shift time constants. Indeed, PC thresholds were low, sometimes submicron, as were threshold shifts. Measurements of instantaneous PC thresholds were thus error prone. (Note that estimates of steady-state threshold shift were much less susceptible to measurement error because these rely on five instantaneous estimates of threshold.) In contrast, the time-course of PC phase adaptation can be reliably measured

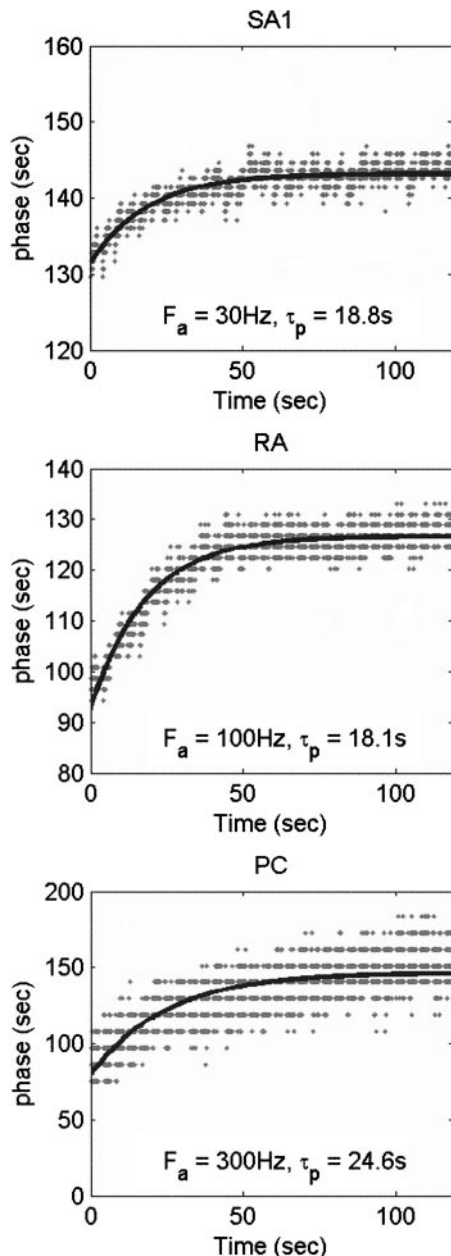


FIG. 7. Impulse phase as a function of time for 1 afferent of each type. Each data point corresponds to the phase of the 1st impulse evoked during a cycle of the adapting stimulus. Dark trace shows the exponential fit to the data. All 3 neurons were nearly perfectly entrained with the stimulus. Digitization in the data reflects temporal resolution of the spike collection system.

because each adaptation run yielded many estimates of the impulse phase, approximately one for each cycle of the adapting stimulus. Furthermore, PC afferents produce very regular entrained responses to high-frequency stimuli (Freeman and Johnson 1982b) so there was little variation (~0.1–0.2 ms) in impulse phase over small time intervals (Fig. 7). In summary, the time-course of phase adaptation for RA and SA1 afferents was comparable with that of I_1 adaptation, as predicted by a simple integrate-and-fire model. We propose that the discrepancy in the time constants obtained for PC threshold and phase adaptation is caused by measurement error in the former.

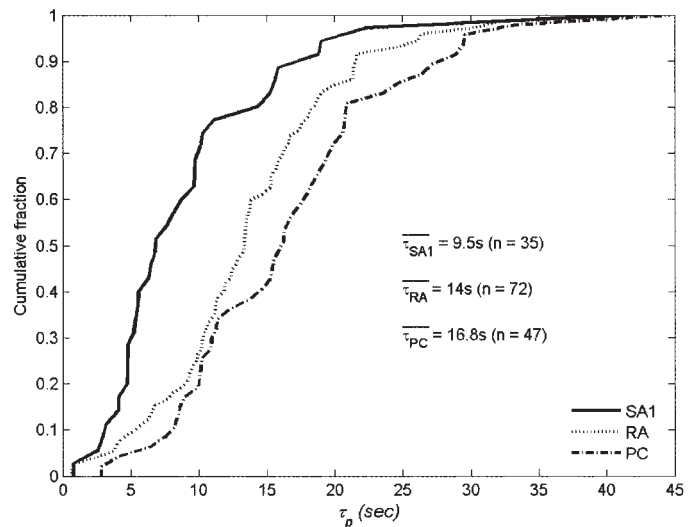


FIG. 8. Cumulative histogram of phase adaptation time constants for the 3 types of fibers. SA1 and RA phase adaptation time constants were similar to their threshold adaptation counterparts, whereas PC time constants were substantially shorter.

Comparing psychophysics and neurophysiology

TIME-COURSE OF ADAPTATION. The time-course of vibrotactile adaptation has been studied in a number of psychophysical studies, either by measuring absolute thresholds at various intervals after the onset of the adapting stimulus (Hahn 1968a,b; Hollins et al. 1990, 1991) or by tracking the subjective intensity of a suprathreshold stimulus over time (Berglund and Berglund 1970; Hahn 1968b). Because psychophysical absolute thresholds depend on a small group of peripheral fibers, perhaps even a single one (Johansson and Vallbo 1979), the time-course of adaptation and recovery of (psychophysical) absolute thresholds is more comparable with that of afferent thresholds than is the time-course of adaptation and recovery of sensation magnitude, which is mediated by a larger population of peripheral fibers. To compare the time-courses of psychophysical and peripheral adaptation, we fitted exponential functions (analogous to that shown in Eq. 1) to the time-courses of psychophysical adaptation obtained from a pair of adaptation studies (Hollins et al. 1990, 1991).

Psychophysical adaptation time constants for adapting frequencies of 10 and 50 Hz varied from ~62 to 212 s (Hollins et al. 1990, 1991). Given that the RA channel is more sensitive than the SA1 channel at all but the lowest frequencies (< approximately 5 Hz; Bolanowski et al. 1988), and that test stimulus frequencies fell within the most sensitive portion of the RA range (10 and 50 Hz), it is the time-course of adaptation within this sensory channel that was likely measured in the two

TABLE 1. τ_a and τ_r constants, in seconds, for absolute and entrainment thresholds, I_0 and I_1

	$\tau_a(I_0)$	$\tau_a(I_1)$	$\tau_r(I_0)$	$\tau_r(I_1)$	τ_p
SA1	11.0	9.0	9.4	17.3	9.5
RA	17.9	13.2	27.0	26.6	14.0
PC	41.8	28.1	20.9	29.6	16.5

The right column, labeled τ_p , shows the phase adaptation time constants. τ_a , mean adaptation; τ_r , recovery time.

threshold-tracking studies, although the PC channel may mediate thresholds at 50 Hz (Hollins et al. 1990, 1991).

In this study, RA adaptation time constants and their PC counterparts estimated from phase data ranged from 1 s to about 40 s (Figs. 4 and 8). If vibrotactile adaptation were exclusively a peripheral phenomenon, psychophysical and afferent thresholds would adapt within a similar time frame. However, the time-course of psychophysical adaptation was much longer than that predicted from our neurophysiological measurements.

TIME-COURSE OF RECOVERY FROM ADAPTATION. To quantify the rate of recovery from psychophysical adaptation, we fitted exponential functions (analogous to that shown in Eq. 2) to psychophysical (absolute) thresholds as they recovered after the termination of the adapting stimulus. These psychophysical recovery time constants ranged from about 26 to 316 s (Gescheider and Wright 1968; Hahn 1968b; Hollins et al. 1990, 1991). Recovery time constants derived from RA fibers ranged from 2 to 45 s. PC recovery time constants ranged from 18 to 92 s. Thus RA and PC time constants were somewhat faster than their psychophysical counterparts but fell within an overlapping range. That psychophysical adaptation and recovery operate on a slower time scale than their counterparts at the sensory periphery suggests central factors contribute to the psychophysical phenomenon.

Neural mechanisms

In the companion paper (Bensmaïa et al. 2005), we propose that adaptation is produced by an influx of ions, probably calcium, through mechanosensitive channels. The increase in concentration of this ion in turn causes a change in the spiking threshold of the afferent or possibly in the transducer gain of the receptor. Because of its dependence on the electrochemical gradient across the receptor membrane, the magnitude of the change in the intracellular concentration of this ion is in part determined by its instantaneous intracellular concentration. The greater the intracellular concentration, the lower the driving force on the ion, and the lower the change in intracellular concentration, and vice versa. The dependence of the change in concentration on the instantaneous concentration is the type of relation that gives rise to an exponential time-course. Thus the ionic hypothesis of adaptation is consistent with its time-course.

The question remains why the time-course of adaptation for entrainment thresholds is different from its absolute threshold counterpart for RA afferents. Similarly, it is unclear why the time-course of I_1 recovery is faster than that of I_0 recovery for SA1 fibers. Within the simple integrate-and-fire framework sketched above, the absolute threshold is proportional to the spiking threshold and inversely proportional to the transducer gain (Bensmaïa et al. 2005)

$$I_0 \propto \frac{T}{k} \quad (5)$$

Thus the only difference between I_0 and I_1 is that one depends on the relative refractoriness of the receptor while the other does not. Differences in the time-courses of I_0 and I_1 adaptation must therefore result from the dynamics of relative refractoriness in the receptor. According to the model, the adapted level

of ΔT (when the afferent has reached steady state) is equal to its preadaptation level in RA afferents (Bensmaïa et al. 2005). One possibility to explain the difference between τ_{I_0} and τ_{I_1} is that the maintenance of ΔT as T changes is a process with a faster time-course than the shift in T itself. Similarly, differences in the rates of I_0 and I_1 recovery in SA1 afferents may be caused by differences in the rates of recovery of T and ΔT . To evaluate these hypotheses, a more detailed biophysical model of mechanoreceptive transduction is required.

What is adaptation?

It is paradoxical that SA1 fibers, named for their slowly declining firing rates in response to a constant indentation, adapt most rapidly to a vibratory stimulus, whereas their rapidly adapting counterparts, RA and PC fibers, adapt to the same stimulus more slowly. Although they unfortunately share the same name, these two kinds of adaptation clearly rely on very different mechanisms. Rapid adaptation to constant indentation is measured in milliseconds and is, at least in the case of PC fibers, determined to a large extent by the mechanical properties of the Pacinian corpuscle (Loewenstein and Skalak 1966). Adaptation to constant vibratory stimulation in the three types of fibers is measured in tens of seconds, which points to a completely different mechanism. For SA1 fibers, vibratory adaptation may be a manifestation of the same mechanism that underlies the slow decline in the response to a constant indentation that inspired their designation; in both cases, ion flow into the receptor may cause the receptor to become desensitized. According to this hypothesis, the time-course of the two types of adaptation should be identical. Figure 9 shows the firing rate evoked in an SA1 afferent by a 1-mm indentation lasting 30 s. The spike rate declines along an approximately exponential time-course with a time constant of 8.4 s, matching its vibratory adaptation counterpart. We recorded the responses of two other SA1 afferents to a step indentation and observed similar time courses (data not shown). We tentatively conclude that, for SA1 afferents, vibratory adaptation and adaptation to a constant indentation reflect the same underlying phenom-

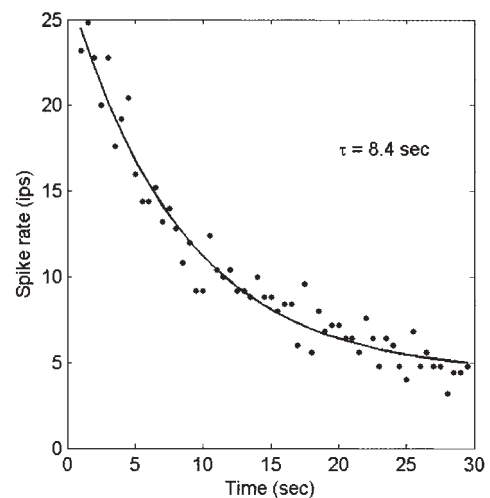


FIG. 9. Decay of the response of an SA1 afferent (averaged in 500-ms bins) to a 1-mm indentation applied over 30 s. Rate of decay of SA1 response is the same as that of SA1 vibratory adaptation, supporting the hypothesis that the same mechanism underlies the 2 phenomena.

non, although more data will be needed to establish this conclusively.

ACKNOWLEDGMENTS

We thank A. Sripati, P. Denchev, and J. Craig for invaluable discussion. We are also indebted to K. Ledoux and M. Hollins for careful reading of the manuscript.

GRANTS

This work was supported by National Institute of Neurological Disorders and Stroke Grants NS-18787, NS-38034, and NS-34086.

REFERENCES

- Bensmaïa SJ, Leung YY, Hsiao SS, and Johnson KO.** Vibratory adaptation of cutaneous mechanoreceptive afferents. *J Neurophysiol* 94: 3024–3037, 2005.
- Berglund U and Berglund B.** Adaptation and recovery in vibrotactile perception. *Percept Mot Skills* 30: 843–853, 1970.
- Bolanowski SJ, Gescheider GA, Verrillo RT, and Checkosky CM.** Four channels mediate the mechanical aspects of touch. *J Acoust Soc Am* 64: 1680–1694, 1988.
- Chubbuck JG.** Small motion biological stimulator. *Johns Hopkins APL Tech Digest* 5: 18–23, 1966.
- Freeman AW and Johnson KO.** A model accounting for effects of vibratory amplitude on responses of cutaneous mechanoreceptors in macaque monkey. *J Physiol* 323: 43–64, 1982a.
- Freeman AW and Johnson KO.** Cutaneous mechanoreceptors in macaque monkey: temporal discharge patterns evoked by vibration, and a receptor model. *J Physiol* 323: 21–41, 1982b.
- Gescheider GA and Wright JH.** Effects of sensory adaptation on the form of the psychophysical magnitude function for cutaneous vibration. *J Exp Psychol* 77: 308–313, 1968.
- Hahn JF.** Low-frequency vibrotactile adaptation. *J Exp Psychol* 78: 655–659, 1968a.
- Hahn JF.** Tactile adaptation. In: *The Skin Senses*, edited by Kenshalo DR. Springfield, IL, Charles C Thomas, 1968b, p 322–330.
- Hollins M, Delemos KA, and Goble AK.** Vibrotactile adaptation on the face. *Percept Psychophys* 49: 21–30, 1991.
- Hollins M, Goble AK, Whitsel BL, and Tommerdahl M.** Time course and action spectrum of vibrotactile adaptation. *Somatosens Mot Res* 7: 205–221, 1990.
- Johansson RS and Vallbo ÅB.** Detection of tactile stimuli. Thresholds of afferent units related to psychophysical thresholds in the human hand. *J Physiol* 297: 405–422, 1979.
- Loewenstein WR and Skalak R.** Mechanical transmission in a Pacinian corpuscle. An analysis and a theory. *J Physiol* 182: 346–378, 1966.
- O'Mara S, Rowe MJ, and Tarvin RP.** Neural mechanisms in vibrotactile adaptation. *J Neurophysiol* 59: 607–622, 1988.
- Talbot WH, Darian-Smith I, Kornhuber HH, and Mountcastle VB.** The sense of flutter-vibration: comparison of the human capacity with response patterns of mechanoreceptive afferents from the monkey hand. *J Neurophysiol* 31: 301–334, 1968.
- Whitsel BL, Kelly EF, Delemos KA, Xu M, and Quibrera PM.** Stability of rapidly adapting afferent entrainment vs responsivity. *Somatosens Mot Res* 17: 13–31, 2000.